nature geoscience

LETTERS

PUBLISHED ONLINE: 26 FEBRUARY 2012 | DOI: 10.1038/NGEO1401

Intra-Panthalassa Ocean subduction zones revealed by fossil arcs and mantle structure

D. G. van der Meer[1,2]*, T. H. Torsvik[3,4,5,6], W. Spakman[1]*, D. J. J. van Hinsbergen[3,6] and M. L. Amaru[1,7]

The vast Panthalassa Ocean once surrounded the supercontinent Pangaea. Subduction has since consumed most of the oceanic plates that formed the ocean floor, so classic plate reconstructions based on magnetic anomalies can be used only to constrain the ocean's history since the Cretaceous period[1,2], and the Triassic–Jurassic plate tectonic evolution of the Panthalassa Ocean remains largely unresolved[3,4]. Geological clues come from extinct intra-oceanic volcanic arcs that formed above ancient subduction zones, but have since been accreted to the North American and Asian continental margins[4]. Here we compile data on the composition, the timing of formation and accretion, and the present-day locations of these volcanic arcs and show that intra-oceanic subduction zones must have once been situated in a central Panthalassa location in our plate tectonic reconstructions[5–7]. To constrain the palaeoposition of the extinct arcs, we correlate them with remnants of subducted slabs that have been identified in the mantle using seismic-wave tomographic models[8,9]. We suggest that a series of subduction zones, together called Telkhinia, may have defined two separate palaeo-oceanic plate systems—the Pontus and Thalassa oceans. Our reconstruction provides constraints on the palaeolongitude and tectonic evolution of the Telkhinia subduction zones and Panthalassa Ocean that are crucial for global plate tectonic reconstructions and models of mantle dynamics.

The spatial uncertainty in reconstructions of oceanic basins increases the further we go back in time, because oceanic plates subduct. Plate reconstructions for the Triassic–Jurassic history of the Panthalassa Ocean, once surrounding the Pangaea supercontinent, are based on the premise that the Pacific plate formed in the Middle Jurassic as a triangle[2], originating from a triple junction between the Farallon, Phoenix and Izanagi plates (Fig. 1). The preserved area of Jurassic palaeoplates represents only a small portion (<10%) of the oceanic crust of the Jurassic Panthalassa Ocean. The remaining part, along with pre-Jurassic oceanic plate configurations, is entirely unconstrained.

However, the geology of the circum-Panthalassa continental margins provides evidence that early Mesozoic subduction-related volcanism occurred in the Panthalassa Ocean[4,10]. On subduction, continental fragments, volcanic arcs, ophiolites and ocean-floor sediments collided with or accreted to the continental margins of, in particular, western North America, far-east Asia and Japan. Marine microfossils in these sediments and palaeomagnetic data constrain their age and palaeolatitude, but their palaeolongitudes remain undetermined. Palaeogeographic reconstructions therefore show uncorrelated intra-Panthalassa exotic terranes essentially unconstrained in the early Mesozoic Panthalassa Ocean[4,11,12]. Notably, some of these terranes preserve relics of fossil Triassic and Jurassic volcanic arc complexes that accreted many tens of millions of years after their extinction to circum-Pacific continents[4,11,13]. This shows that Triassic and Jurassic subduction zones existed away from continental margins in the Panthalassa Ocean. As subducted slab remnants (that is, subducted oceanic crust and lithosphere) associated with these subduction zones might still reside in the lower mantle, the structure of the sub-Pacific mantle may provide palaeolongitudes of intra-oceanic subduction, allowing significant improvement of plate tectonic reconstructions of the early Mesozoic Panthalassa Ocean.

We first explore the geological evidence for the locations of these intra-oceanic subduction zones. The best-constrained exotic terranes with intra-Panthalassa volcanic arc remnants of Triassic–Jurassic age are the Kolyma–Omolon superterrane (northeast Asia)[4,14,15], the Anadyr–Koryak terrane (east Asia)[4,16,17], the Oku–Niikappu terrane (Japan)[13] and the Wrangellia and Stikinia terranes (western North America)[4,18] (Fig. 1).

Kolyma–Omolon consists of the cratonic Omulevka and Omolon terranes, which rifted away from Siberia in the Carboniferous period[4,14], and is associated with a fossil Triassic–Jurassic subduction complex of arc volcanics, accretionary wedges and ophiolite belts[4,14]. Palaeomagnetic data[4,14] indicate that the Omulevka and Omolon terranes remained stationary at 40°–55° N in Permian–Triassic times, followed by rapid northward motion until the Late Jurassic–Early Cretaceous collision with Siberia at high polar latitudes[4,14,15].

Radiolarian assemblages from Mesozoic exotic terranes in Anadyr–Koryak (Fig. 1) indicate that they represent an amalgamation of rocks deposited at different palaeolatitudes, spanning a latitudinal width greater than 3,000 km (ref. 17). Within these terranes, Middle–Upper Triassic arc volcanics and back-arc and fore-arc basin sediments are separated from an overlying Middle Jurassic to Upper Cretaceous sequence of similar facies[16,17] by a Lower–Middle Jurassic deep-oceanic radiolarian-bearing sequence without evidence for volcanism[17]. Taxonomic composition of the radiolarian assemblages indicate that the second-generation island arc complex was formed ~2,000 km away from the Asian continental margin[17]. Faunal[17] and palaeomagnetic data[4,16] show that the exotic terranes formed at low latitudes between ~20° and 40° N (refs 4,16,17) from Triassic to earliest Cretaceous times, followed by a northward drift culminating Early–Middle Cretaceous accretion to the east Asian continental margin at high latitudes[4,16,17].

Japan's accretionary wedge formed episodically over the past 500 million years (Myr)[10] and contains rocks of an intra-oceanic

[1]Institute of Earth Sciences, Utrecht University, Budapestlaan 4, 3584 CD Utrecht, The Netherlands, [2]Nexen Petroleum UK Ltd, Charter Place, Vine Street, Uxbridge, Middlesex UB8 1JG, UK, [3]Physics of Geological Processes, University of Oslo, NO-0316 Oslo, Norway, [4]Center for Geodynamics, Geological Survey of Norway, NO-7494 Trondheim, Norway, [5]School of Geosciences, University of the Witwatersrand, WITS 2050 Johannesburg, South Africa, [6]Center for Advanced Study, Norwegian Academy of Science and Letters, Drammensveien 78, NO-0271 Oslo, Norway, [7]Chevron Energy Technology Company, 1500 Louisiana St, Houston, Texas 77002, USA. *e-mail: douwevdm@gmail.com; wims@geo.uu.nl.

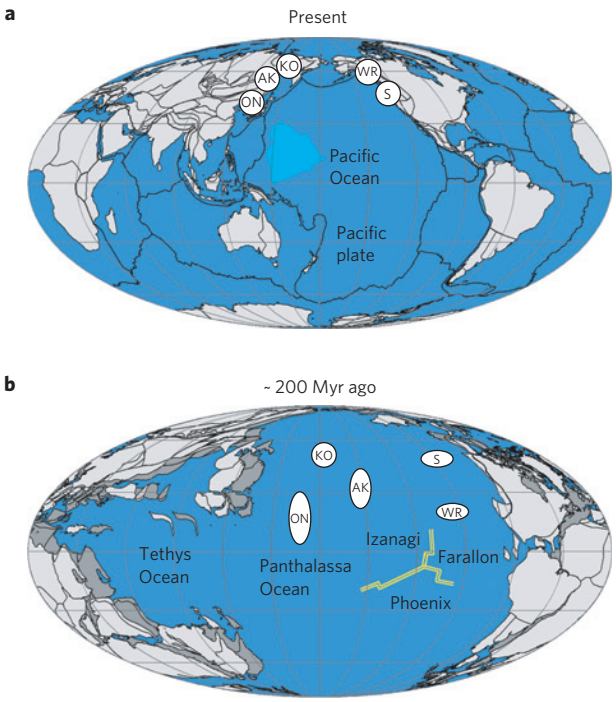

Figure 1 | Present understanding of the Panthalassa Ocean. Modified plate tectonic reconstruction[5–7] centred at the 180° meridian at **a**, the present time and **b**, 200 Myr ago (earliest Jurassic). Continental blocks in absolute plate reference frames: slab-fitted frame[7], light grey; hybrid true-polar-wander-corrected frame[5,6,22], dark grey. Light blue denotes preserved Jurassic (140–175 Myr old) old crust of the Pacific plate. Yellow zigzag shows the presumed spreading ridge. White ellipses represent terranes: AK, Anadyr–Koryak; KO, Kolyma–Omolon; ON, Oku–Niikappu; S, Stikinia; WR, Wrangellia.

volcanic arc in the Oku–Niikappu region[13]. The Oku–Niikappu arc is overlain by Upper Jurassic–Lower Cretaceous (~145–130 Myr old) radiolarites, marking the minimum age of arc extinction, and Middle-Cretaceous (~105–95 Myr old) foreland basin clastic deposits, marking the arrival at Japan's subduction zone. The Oku–Niikappu arc had thus been extinct for at least 40 Myr at the moment of accretion to Japan, indicating that the intra-oceanic subduction zone from which it was derived was located far offshore east Asia[13]. Palaeomagnetic[19,20] and biostratigraphic[21] data from Triassic and Jurassic rocks in the Japanese accretionary prism consistently show derivation from equatorial to low latitudes (~5°–30° N; refs 19–21), indicating that the plate on which the Oku–Niikappu arc formed had a northward component of motion after extinction. We thus infer a Middle-Jurassic low northerly palaeolatitude for the Oku–Niikappu arc.

Finally, the Stikinia and Wrangellia terranes of western North America form an amalgamation of Permian–Jurassic intra-oceanic arcs, ophiolites and accretionary wedges that formed somewhere west of continental North America. Palaeomagnetic data constrain the Late-Triassic palaeolatitude of Wrangellia to ~20° N (refs 4,18), south of Stikinia (~30°–40° N; ref. 4), and a northward drift by oblique and margin-parallel motion relative to north America in Cretaceous and younger time[4,18].

Together, these exotic terranes document that intra-oceanic subduction zones existed far offshore from the circum-Pacific continental margins in Triassic and Early Jurassic time, spread over latitudes from near-equatorial to ~55° N. We now explore plate tectonic reconstructions in a mantle reference frame and seismic tomographic models to identify where slab-like anomalies reside that may constrain the palaeolongitudes of these subduction zones.

To estimate the position of possible remnants of intra-Panthalassa Ocean subduction relative to the circum-Panthalassa continents in Triassic–Early Jurassic time, we place our global plate tectonic reconstruction[5] in a mantle reference frame. For the early Mesozoic, there are no hotspot reference frames[6], but we can resort to two alternatives, a hybrid true-polar-wander-corrected reference frame[5,6,22] or our slab-fitted frame[7], which is a modification of the former. The reference frames constrain the longitudes of the early Mesozoic Panthalassa Ocean (Fig. 1b), a region largely occupied by the present Pacific Ocean (Fig. 1a). This provides the required search area at the surface, where remnants of intra-Panthalassa subduction should reside in the mantle.

To predict the depth range at which Triassic–Jurassic slabs reside in the mantle, we can use estimates of global average rates of slab sinking. Based on previous correlations between tomographic interpretation of subducted slabs and the geological record[7,23], the studied lower-mantle slabs indicate sinking rates of ~1 cm yr^{-1}. Mantle-convection modelling[24,25] correlated with global tomographic models obtain the best fit when higher sinking rates (>1.5 cm yr^{-1}) are used. We assume average slab-sinking rates are at least 1 cm yr^{-1} in the mantle, hence early Mesozoic subducted slabs originating from the Panthalassa Ocean should reside in the lower half of the Pacific mantle (>1,500 km depth) at present. There, the tomographic P-wave speed model (UU-P07; ref. 8) shows an elongated zone of segmented positive anomalies from 30° S to 60° N below the central Pacific Ocean, at depths greater than 1,900 km (Figs 2 and 3; Supplementary Movies, Figs S1–S8). At 50° N this elongated zone curves northeastwards, towards anomalies that have previously been interpreted by us as slabs associated with Mesozoic intra-oceanic subduction west of North America[7], associated with the Wrangellia and Stikinia terranes (Fig. 1). Previously, the presence of seismic scatterers (Fig. 2) in the deep mantle below the central Pacific was interpreted to be caused by remnants of subducted and folded former oceanic crust[26].

The north–south belt of positive anomalies is well corroborated by a recent tomographic S-wave speed model (S40RTS; ref. 9) that is based on independent data and methodology. This model shows fairly similar lateral geometry at depths of 1,800–2,400 km (Fig. 3; Supplementary Movies). Both models indicate a separation of the top part of the Pacific large low shear wave velocity province (LLSVP; ref. 27) into two parts to a depth of ~2,700 km (Fig. 3; Supplementary Movies). Waveform modelling of trans-Pacific S-wave seismic rays[28] along a northwest–southeast profile also corroborates our findings, where at depths greater than ~2,550 km, the geometry of the Pacific LLSVP consists of two modelled highs, separated by a 740-km-wide gap[28]. At 2,400 km depth (Fig. 3b) the modelled southeastern edge of the western LLSVP high[28] terminates at the north–south belt of positive anomalies.

In both mantle reference frames[7,22], the early Mesozoic Laurentian, east Asian and southern Gondwana continental margins are placed above the corresponding Farallon[7,29], east China[7,23] and Georgia Islands slabs[7] (Fig. 4). The anomalies identified in the deep mantle below the Pacific Ocean (Figs 2 and 3) do not project below any continental margin in the reconstruction (Fig. 4; Supplementary Figs S1–S8), but instead have an intra-Panthalassa location. This central-Pacific belt of anomalies is therefore interpreted as the remnant of intra-Panthalassa subduction and constrains the location of the Triassic–Early Jurassic intra-Panthalassa subduction zones that are recorded in the circum-Pacific exotic terranes.

This interpretation is consistent with the palaeolatitudes from near-equatorial to ~55° N recorded in the Japanese and far-east Asian terranes[4,13,14,16,17]. In both tomographic models[8,9] (Fig. 3), the amplitudes of the anomalies are weaker than for other slabs identified at equivalent depths associated with circum-Pangaea subduction zones[7]. This may be explained by the proximity of the slabs to the hotter LLSVP (ref. 27), where enhanced thermal

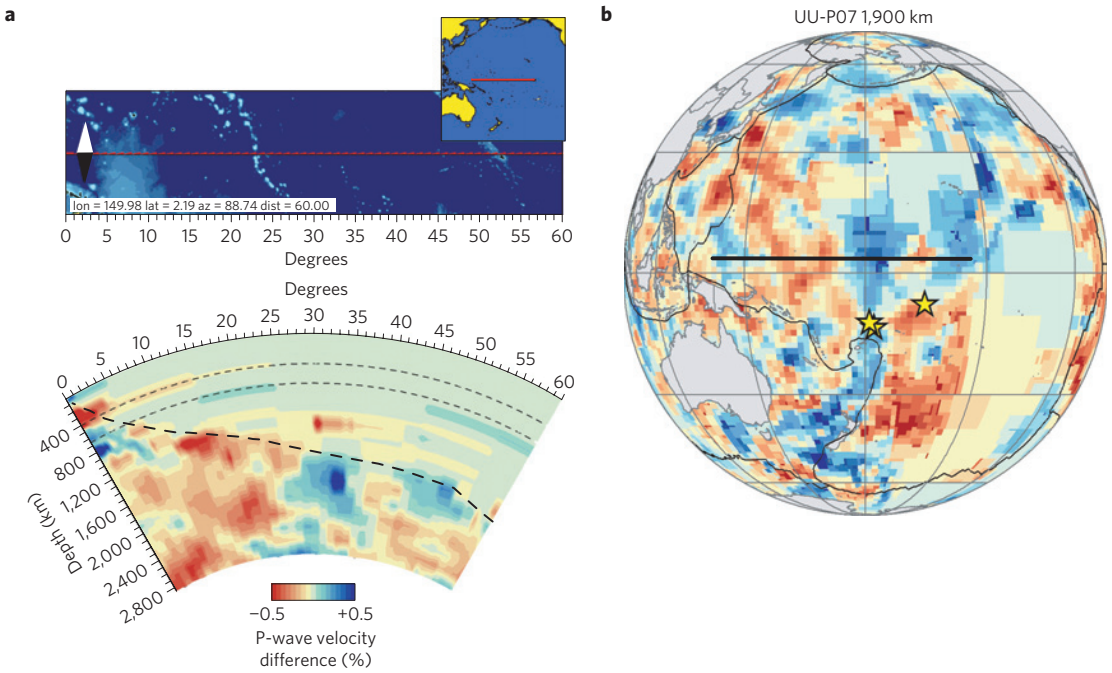

Figure 2 | Tomographic slices. Two cross-sections of the tomographic model[8] centred at the 180° meridian of **a**, vertical slice at 4° N and **b**, horizontal slice at 1,900 km depth. Fast (blue) P-wave speed anomalies at the centre of each tomography section show the suggested Triassic–Jurassic slab remnants. Yellow stars represent central Pacific seismic scatterers, caused by subducted and folded oceanic crust[26]. Zones of low- or absent image resolution occur above the inclined large-dashed line in the lower panel of **a**. Numbers along the horizontal axis in **a** denote arc-degrees along the section. The horizontal solid black line in **b** shows the location of section **a**.

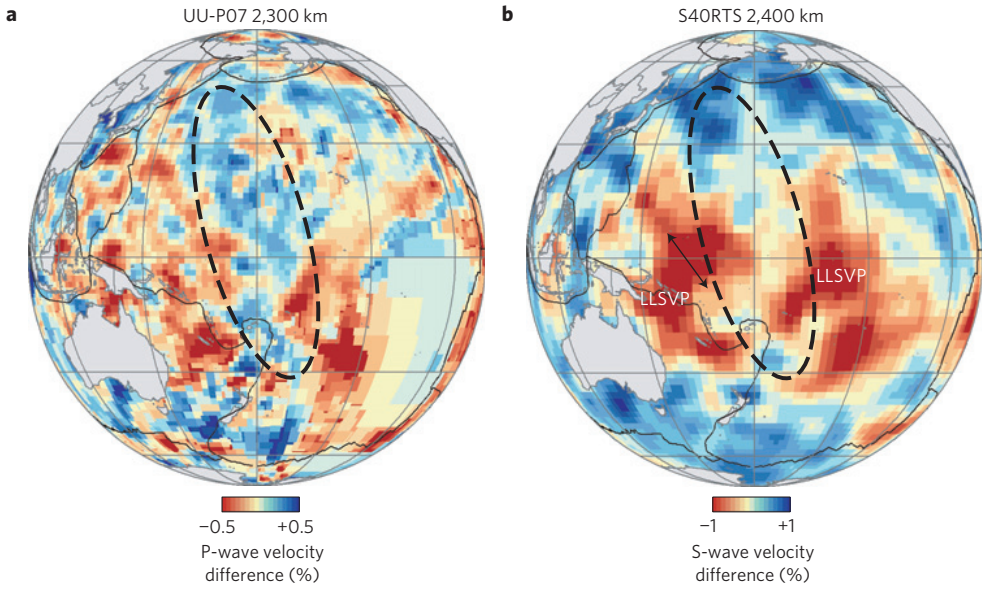

Figure 3 | Comparison of tomographic models. Tomographic slice **a**, at 2,300 km depth[8], showing positive P-wave speed anomalies below the central Pacific, depicted here by black dashed oval, and **b**, at 2,400 km depth[9], showing S-wave speed anomalies[9] with zero to positive S-wave speed amplitudes, separating the LLSVP with strong negative amplitude into a western and eastern region. Black arrow shows the modelled extent of the western LLSVP high along a northwest–southeast profile[28].

assimilation of the slab may combine with lower tomographic resolution to reduce seismic velocity anomalies.

The zone of anomalies is not continuous. This may imply strongly segmented plate boundaries in the Triassic–Jurassic Panthalassa (Figs 2 and 4), perhaps owing to their subduction history (for example, because of the opening of back-arc basins) similar to Mesozoic–Cenozoic subduction configurations of the northern Tethys Ocean[7] and the west Pacific Ocean at present.

Using the palaeolatitude constraints and their position with respect to each other, we suggest that the Wrangellia and Stikinia intra-oceanic terranes were located outboard of western Laurentia, and are associated with slabs that are found to the west of the Farallon slab[7,29] (Fig. 4). We correlate the Kolyma–Omolon, Anadyr–Koryak and Oku–Niikappu subduction-related exotic terranes to the array of central-Pacific anomalies (Fig. 4). To bring these arcs from a central-Pacific origin to the continental margin

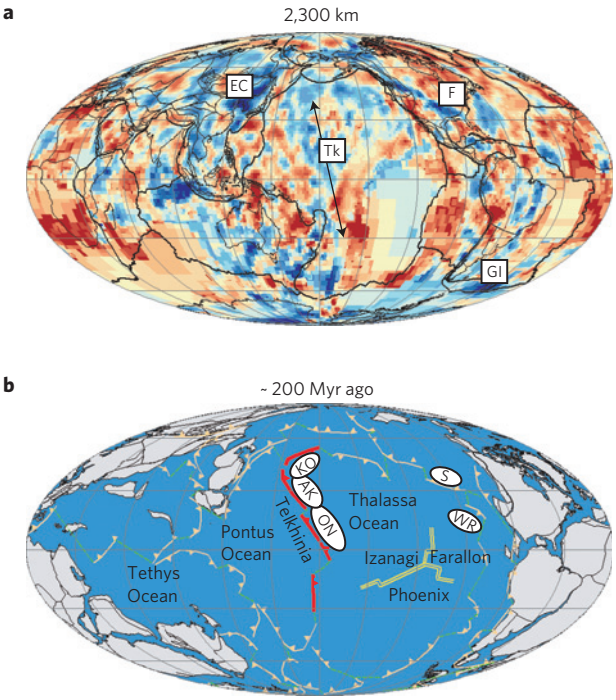

Figure 4 | Plate tectonic interpretation of tomography. a, Tomographic[8] depth slice at 2,300 km. Colour scale as in Fig. 3. Discussed slabs: EC, east China; F, Farallon; GI, Georgia Islands; Tk, Telkhinia slab group. **b**, Modified plate tectonic reconstruction[5–7] 200 Myr ago (Jurassic–Triassic boundary). Red lines with triangles denote interpreted subduction zones, polarities are speculative. Yellow zigzag denotes presumed spreading ridge. Green line denotes presumed transform zone. White ellipses denote inferred position of the discussed exotic terranes (see also Fig. 1).

after their extinction requires plate speeds not exceeding 10 cm yr^{-1}, which is comparable to modern plate velocities.

If we assume that all main positive anomalies represent slab remnants, their overall configuration (Fig. 4; Supplementary Figs S1–S8) implies a major division of the early Mesozoic Panthalassa Ocean into a western and eastern realm, separated by a north–south trending belt of intra-oceanic subduction zones. We name the eastern part the Thalassa Ocean(s), hosting the preserved parts of the Izanagi, Pacific, Phoenix and Farallon plates. The western part we denote Pontus Ocean, of which all its oceanic lithosphere has been subducted. The dividing array of intra-oceanic subduction zones we name Telkhinia. We tentatively place the Japanese and Asian exotic terranes on the western margin of the Thalassa oceanic plate(s). The two major Pontus and Thalassa oceans are surrounded by smaller peripheral oceans including the Mezcalera Ocean[30] in the east, the Slide Mountain Ocean[4] in the northeast, the Oimyakon Ocean[4] in the north and Mongol–Okhotsk Ocean[23] in the northwest. In the west a transition to the Tethys Ocean seems to occur through a number of undocumented subduction zones.

Assimilating these constraints in our reconstruction[5–7] allows for the following, consistent reconstruction. Intra-oceanic subduction along Telkhinia from the Triassic to Early Jurassic led to the formation of island arcs, partly preserved at circum-Pacific continental margins[4,13–17], and led to slab remnants below the central Pacific Ocean, identified in tomographic models[8,9] from medium latitudes in the south to high latitudes in the north. Our reconstructed position of the Telkhinia subduction zones provides a new estimate for the palaeolongitude of the associated superterranes and yields new insights in the geodynamic evolution of the Panthalassa Ocean. This provides first-order constraints for more detailed plate tectonic reconstructions of oceanic domains of the early Mesozoic, and allows for the building of more realistic geodynamic models derived from those.

Methods

Geological descriptions and palaeomagnetic data of fossil volcanic arcs of the circum-Pacific margins were tested against criteria (Triassic–Jurassic fossil arc, exotic fauna, accretion time) for a central Panthalassa Ocean intra-oceanic subduction zone.

Hit counts (Supplementary Fig. S9) of the tomographic model[8] show that in our area of interest (30° S–60° N), the mantle is sampled with hit counts varying from ~500 raypaths per cell to ~5,000 raypaths per cell. Spike tests as indicators of spatial resolution quality (Supplementary Fig. S10), show that anomaly sign patterns on scales of 500–1,000 km are detectable in the lower mantle below the central Pacific mantle where the cell hit count is >500 (outside the low-resolution zones, indicated by dashed outlines in Supplementary Figs S1–S8 and S10). The spike tests indicate that anomalies of 500–1,000 km are detectable, but their amplitudes are underestimated. We selected only imaged anomalies in the UU-P07 tomographic model[8], with peak amplitudes above +0.2%, consistent with our previous efforts of global slab identification for constraining the longitudes of Pangaea in an absolute mantle reference frame[7].

Palaeosubduction zones were added based on the tomographic interpretation to the plate tectonic reconstruction[5–7] (Fig. 4; Supplementary Figs S1–S8). The error in palaeosubduction location was estimated to be ±500 km for the anomalies in the lower mantle[7].

We tentatively correlate slab windows between subduction-zone segments to transfer zones. These remain speculative, as the apparent slab windows could also be the result of ridge subduction or tomographic imaging.

Nomenclature of the Panthalassa Ocean subdivision (Fig. 4; Supplementary Figs S1–S8) has been based on Greek mythology for consistency with the Greek word Panthalassa ('all sea'). The offspring of the primeval gods Pontus and Thalassa were the Telkhines, who were later cast by Zeus to the underworld.

Received 25 August 2011; accepted 18 January 2012; published online 26 February 2012

References

1. Engebretson, D. C., Cox, A. & Gordon, R. G. Relative motions between oceanic and continental plates in the Pacific Basin. *Geol. Soc. Am. Spec. Pap.* **206,** 1–59 (1985).
2. Müller, R. D., Sdrolias, M., Gaina, C., Steinberger, B. & Heine, C. Long-term sea-level fluctuations driven by ocean basin dynamics. *Science* **319,** 1357–1362 (2008).
3. Nur, A. & Ben-Avraham, Z. Lost Pacifica continent. *Nature* **270,** 41–43 (1977).
4. Nokleberg, W. J. *et al.* Phanerozoic tectonic evolution of the circum-north Pacific. *USGS Prof. Pap.* **1626,** 1–122 (2000).
5. Torsvik, T. H., Müller, R. D., Van der Voo, R., Steinberger, B. & Gaina, C. Global plate motion frames: Toward a unified model. *Rev. Geophys.* **46,** 1–44 (2008).
6. Steinberger, B. & Torsvik, T. H. Absolute plate motions and true polar wander in the absence of hotspot tracks. *Nature* **452,** 620–624 (2008).
7. van der Meer, D. G., Spakman, W., van Hinsbergen, D. J. J., Amaru, M. L. & Torsvik, T. H. Towards absolute plate motions constrained by lower-mantle slab remnants. *Nature Geosci.* **3,** 36–40 (2010).
8. Amaru, M. L. *Global Travel Time Tomography with 3-D Reference Models* PhD thesis, Utrecht Univ. (2007).
9. Ritsema, J., Deuss, A., van Heijst, H. J. & Woodhouse, J. H. S40RTS: A degree-40 shear-velocity model for the mantle from new Rayleigh wave dispersion, teleseismic traveltime and normal-mode splitting function measurements. *Geophys. J. Int.* **184,** 1223–1236 (2011).
10. Isozaki, Y., Maruyama, S. & Furuoka, F. Accreted oceanic materials in Japan. *Tectonophysics* **181,** 179–205 (1990).
11. Shi, G. R. The marine Permian of east and northeast Asia: An overview of biostratigraphy, palaeobiogeography and palaeogeographical implications. *J. Asian Earth Sci.* **26,** 175–206 (2006).
12. Golonka, J. Late Triassic and Early Jurassic palaeogeography of the world. *Palaeogeogr. Palaeoclimatol. Palaeoecol.* **244,** 297–307 (2007).
13. Ueda, H. & Miyashita, S. Tectonic accretion of a subducted intraoceanic remnant arc in Cretaceous Hokkaido, Japan, and implications for evolution of the Pacific northwest. *Island Arc* **14,** 582–598 (2005).
14. Stone, D. B., Minyuk, P. & Kolosev, E. New paleomagnetic paleolatitudes for the Omulevka terrane of northeast Russia: A comparison with the Omolon terrane and the eastern Siberian platform. *Tectonophysics* **377,** 55–82 (2003).
15. Oxman, V. S. Tectonic evolution of the Mesozoic Verkhoyansk–Kolyma belt (NE Asia). *Tectonophysics* **365,** 45–76 (2003).
16. Harbert, W. *et al.* Reconnaissance paleomagnetism of Late Triassic blocks, Kuyul region, northern Kamchatka Peninsula, Russia. *Tectonophysics* **361,** 215–227 (2003).
17. Filatova, N. I. & Vishnevskaya, V. S. Radiolarian stratigraphy and origin of the Mesozoic terranes of the continental framework of the northwestern Pacific (Russia). *Tectonophysics* **269,** 131–150 (1997).

18. Kent, D. V. & Irving, E. Influence of inclination error in sedimentary rocks on the Triassic and Jurassic apparent pole wander path for North America and implications for Cordilleran tectonics. *J. Geophys. Res.* **115,** B10103 (2010).
19. Oda, H. & Suzuki, H. Paleomagnetism of Triassic and Jurassic red bedded chert of the Inuyama area, central Japan. *J. Geophys. Res.* **105,** 25743–25767 (2000).
20. Uno, K., Furukawa, K. & Hada, S. Margin-parallel translation in the western Pacific: Paleomagnetic evidence from an allochthonous terrane in Japan. *Earth Planet. Sci. Lett.* **303,** 153–161 (2011).
21. Matsuoka, A. Late Jurassic tropical Radiolaria: Vallupus and its related forms. *Palaeogeogr. Palaeoclimatol. Palaeoecol.* **119,** 359–369 (1996).
22. Torsvik, T. H., Burke, K., Steinberger, B., Webb, S. J. & Ashwal, L. D. Diamonds sampled by plumes from the core-mantle boundary. *Nature* **466,** 352–355 (2010).
23. van der Voo, R., Spakman, W. & Bijwaard, H. Mesozoic subducted slabs under Siberia. *Nature* **397,** 246–249 (1999).
24. Lithgow-Bertollini, C. & Silver, P. G. Dynamic topography, plate driving forces and the African superswell. *Nature* **395,** 269–272 (1998).
25. Steinberger, B. Slabs in the lower mantle—results of dynamic modelling compared with tomographic images and the geoid. *Phys. Earth Planet. Int.* **118,** 241–257 (2000).
26. Kaneshima, S. & Helffrich, G. Small scale heterogeneity in the mid-lower mantle beneath the circum-Pacific area. *Phys. Earth Planet. Int.* **183,** 91–103 (2010).
27. Garnero, E. J. & McNamara, A. K. Structure and dynamics of Earth's lower mantle. *Science* **320,** 626–628 (2008).
28. He, Y. & Wen, L. Structural features and shear-velocity structure of the Pacific Anomaly. *J. Geophys. Res.* **114,** B02309 (2009).
29. Grand, S., van der Hilst, R. D. & Widiyantoro, S. Global seismic tomography: A snapshot of convection in the earth. *GSA Today* **7,** 1–7 (1997).
30. Dickinson, W. R. & Lawton, T. F. Carboniferous to Cretaceous assembly and fragmentation of Mexico. *Geol. Soc. Am. Bull.* **113,** 1142–1160 (2001).

Acknowledgements

D.G.v.d.M. thanks the Geological Survey of Norway for its hospitality during his sabbatical, D. Stone for the discussions on regional geology and P. Cawood, L. Liu and J. B. Murphy for reviews. Part of this work was conducted under programmes of the Vening Meinesz School of Geodynamics (Utrecht University) and the Netherlands Research Centre of Integrated Solid Earth Sciences. T.H.T. and D.J.J.v.H. acknowledge financial support from Statoil (SPlates Model project). T.H.T. acknowledges the European Research Council under the European Union's Seventh Framework Programme (FP7/2007-2013)/ERC Advanced Grant Agreement Number 267631 (Beyond Plate Tectonics). This paper contributes to the ESF EUROCORES programme TOPO-EUROPE.

Author contributions

D.G.v.d.M. carried out the slab identification and plate tectonic reconstruction modifications. W.S. co-developed the tomographic model. T.H.T. provided the plate tectonic reconstructions. D.J.J.v.H. provided integration between surface geology, orogenesis and subduction. M.L.A. developed the tomographic model as part of her PhD work at Utrecht University. All authors shared in writing the article.

Additional information

The authors declare no competing financial interests. Supplementary information accompanies this paper on www.nature.com/naturegeoscience. Reprints and permissions information is available online at www.nature.com/reprints. Correspondence and requests for materials should be addressed to D.G.v.d.M. or W.S.

nature geoscience

SUPPLEMENTARY INFORMATION

DOI: 10.1038/NGEO1401

Intra-Panthalassa Ocean subduction zones revealed by fossil arcs and mantle structure

DOI: 10.1038/NGEO1401

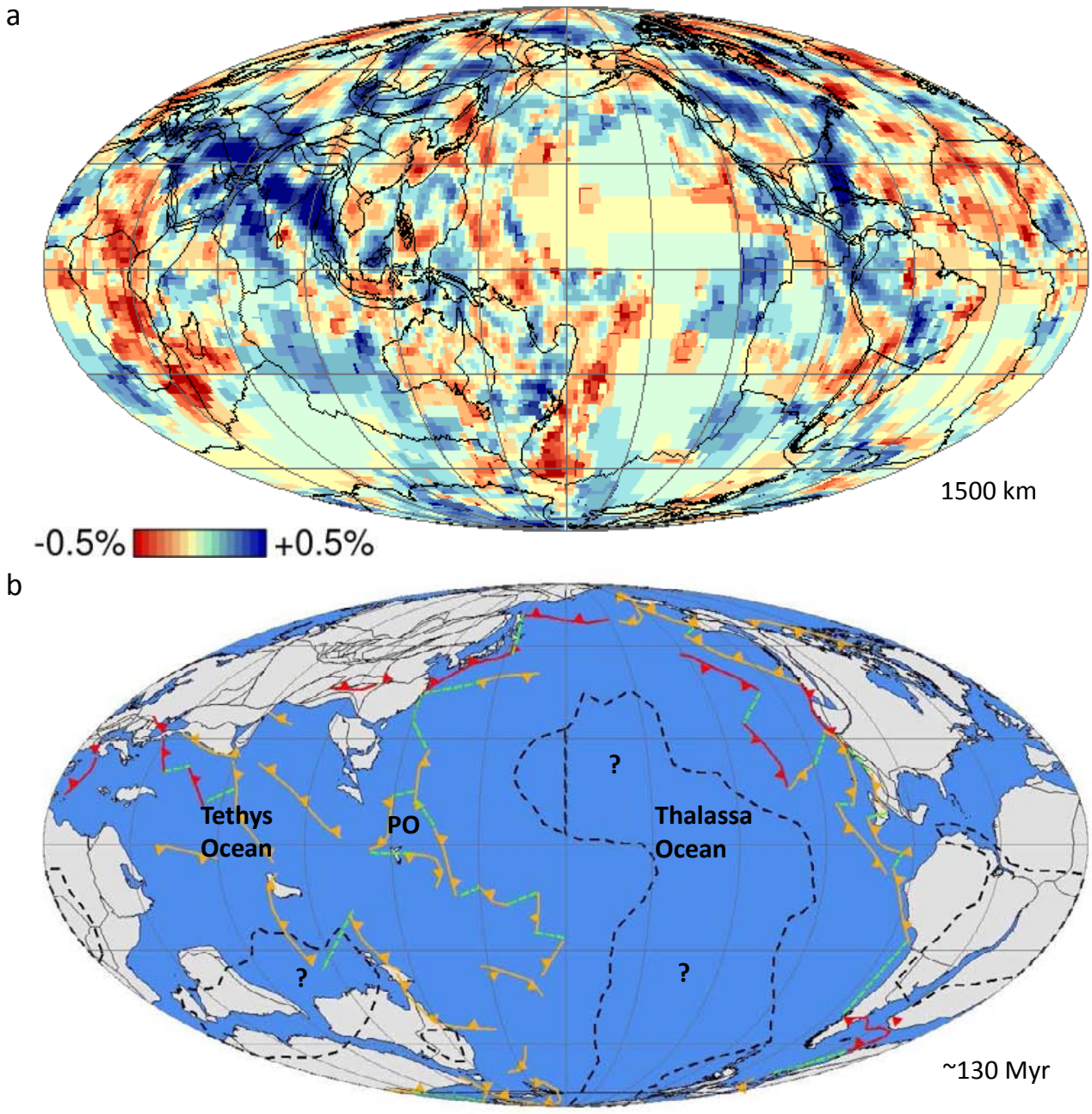

Supplementary Figure 1 Plate tectonic interpretation of tomography. Mollweide projection of a) tomographic depth slice with present-day plate boundaries and continents at 1500 km depth and corresponding b) plate tectonic interpretation at ~130 Myr. Continental blocks in grey, Dashed outline: Low resolution zone as based on spike tests (Supplementary Figure 2). Red line with triangles: previously described subduction zones (van der Meer et al. 2010). Orange line with triangles: other subduction zones. Green line: Presumed transform zone.

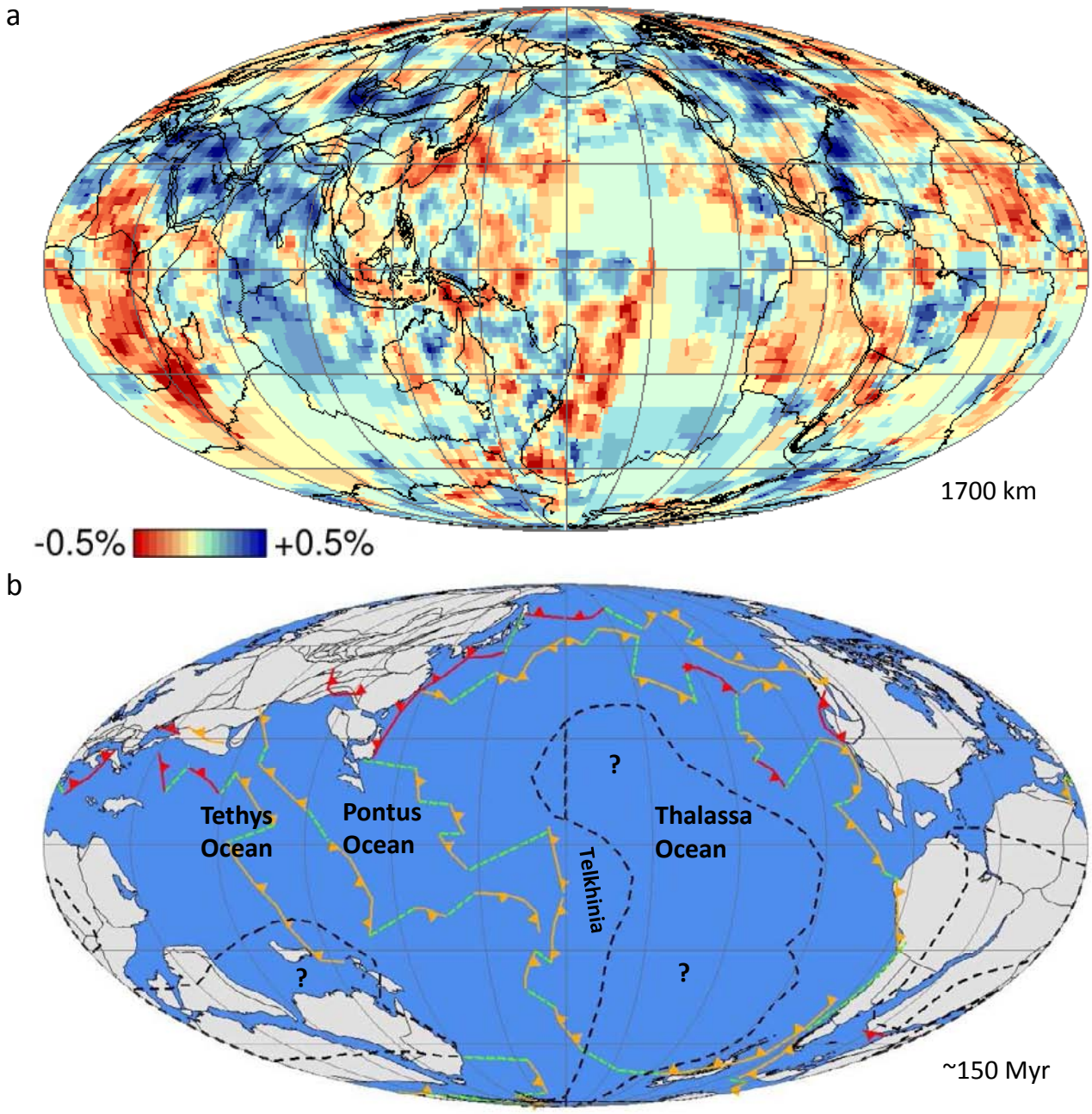

Supplementary Figure 2 Plate tectonic interpretation of tomography. Mollweide projection of a) tomographic depth slice with present-day continents at 1700 km and b) plate tectonic interpretation at ~150 Myr. Legend similar as in Supplementary Figure 1.

DOI: 10.1038/NGEO1401

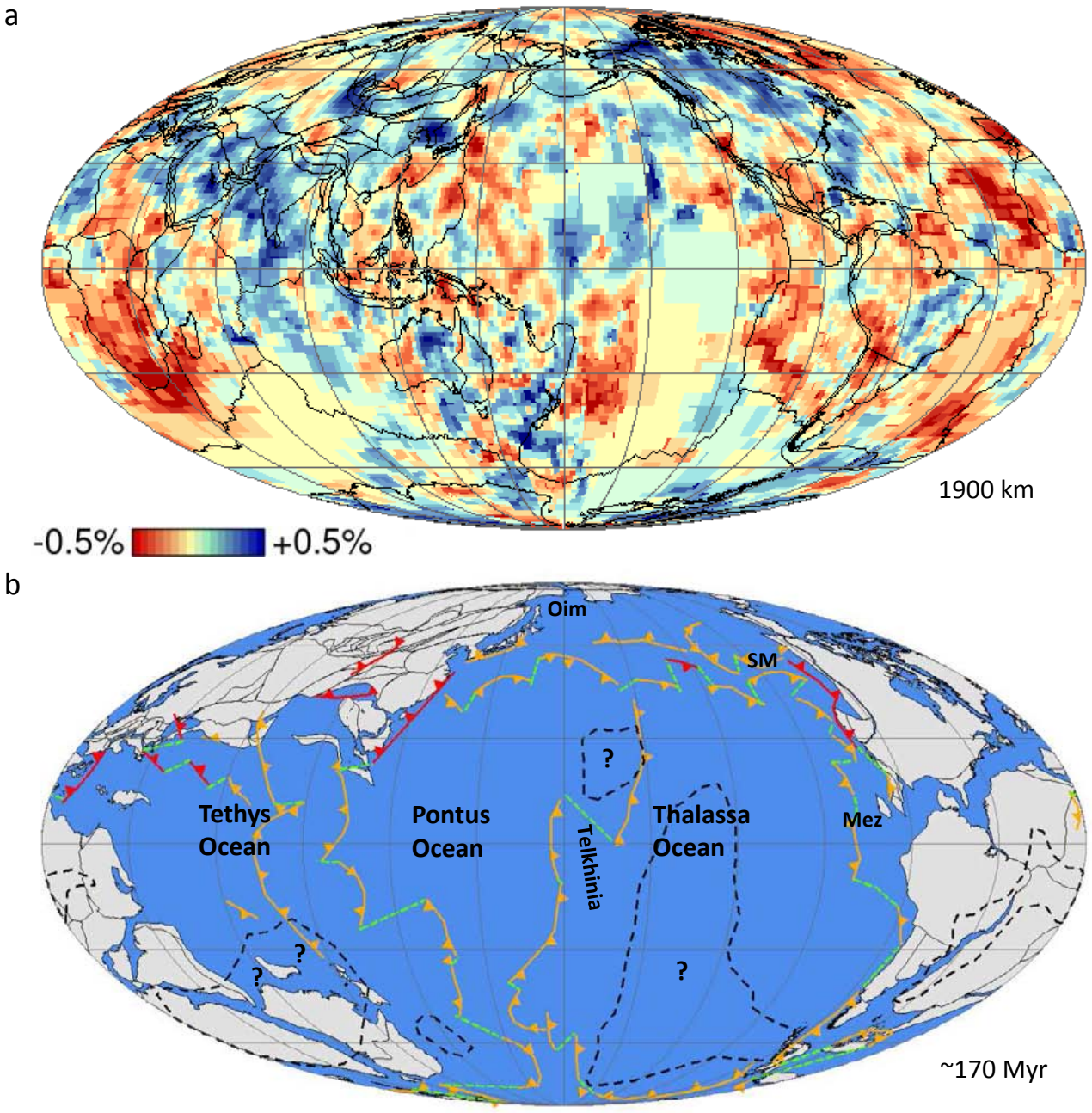

Supplementary Figure 3 Plate tectonic interpretation of tomography. Mollweide projection of a) tomographic depth sliceswith present-day continents at 1900 km and b) plate tectonic interpretation at ~170 Myr. Legend similar as in Supplementary Figure 1.

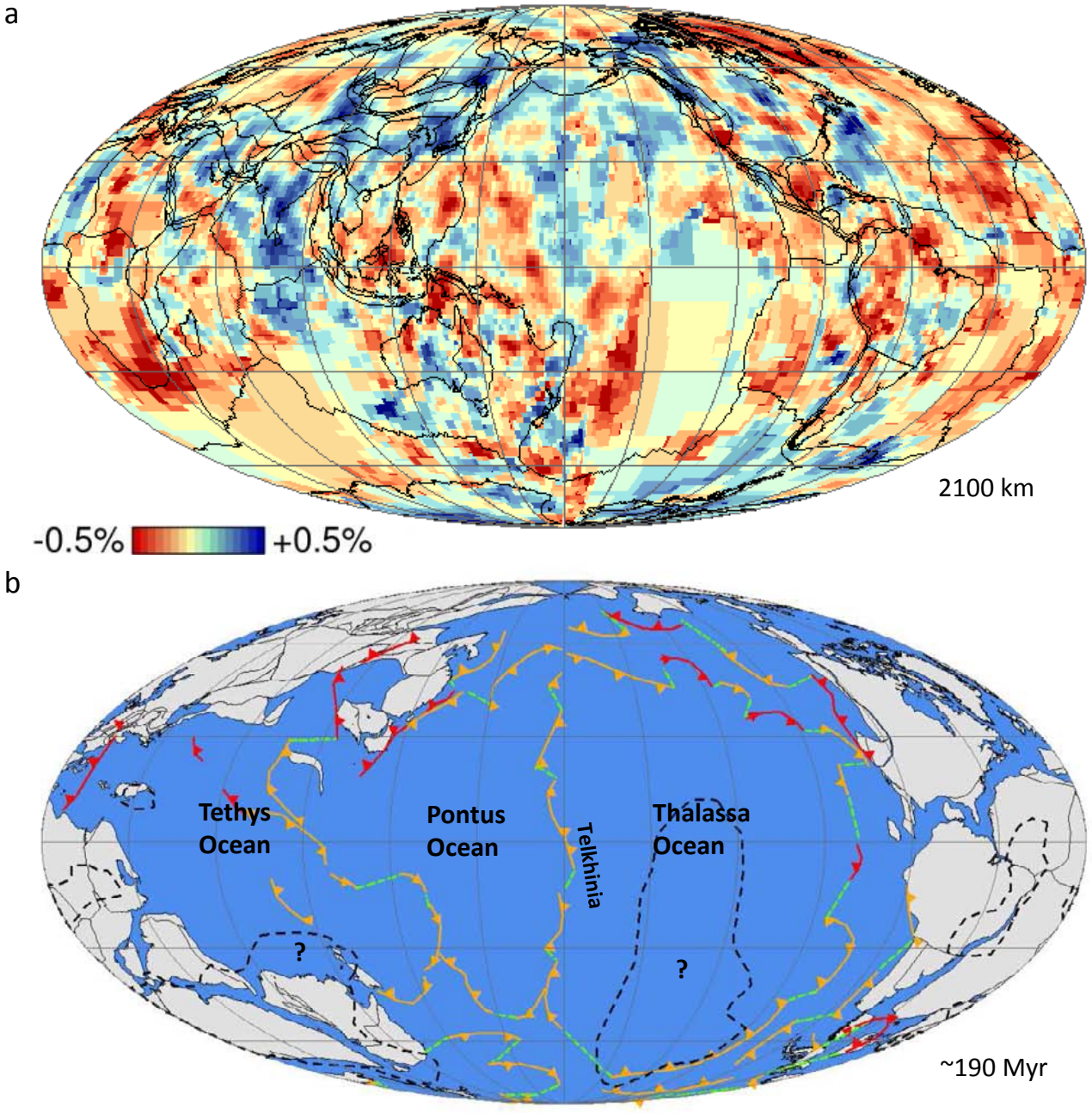

Supplementary Figure 4 Plate tectonic interpretation of tomography. Mollweide projection of a) tomographic depth sliceswith present-day continents at 2100 km and b) plate tectonic interpretation at ~190 Myr. Legend similar as in Supplementary Figure 1.

DOI: 10.1038/NGEO1401

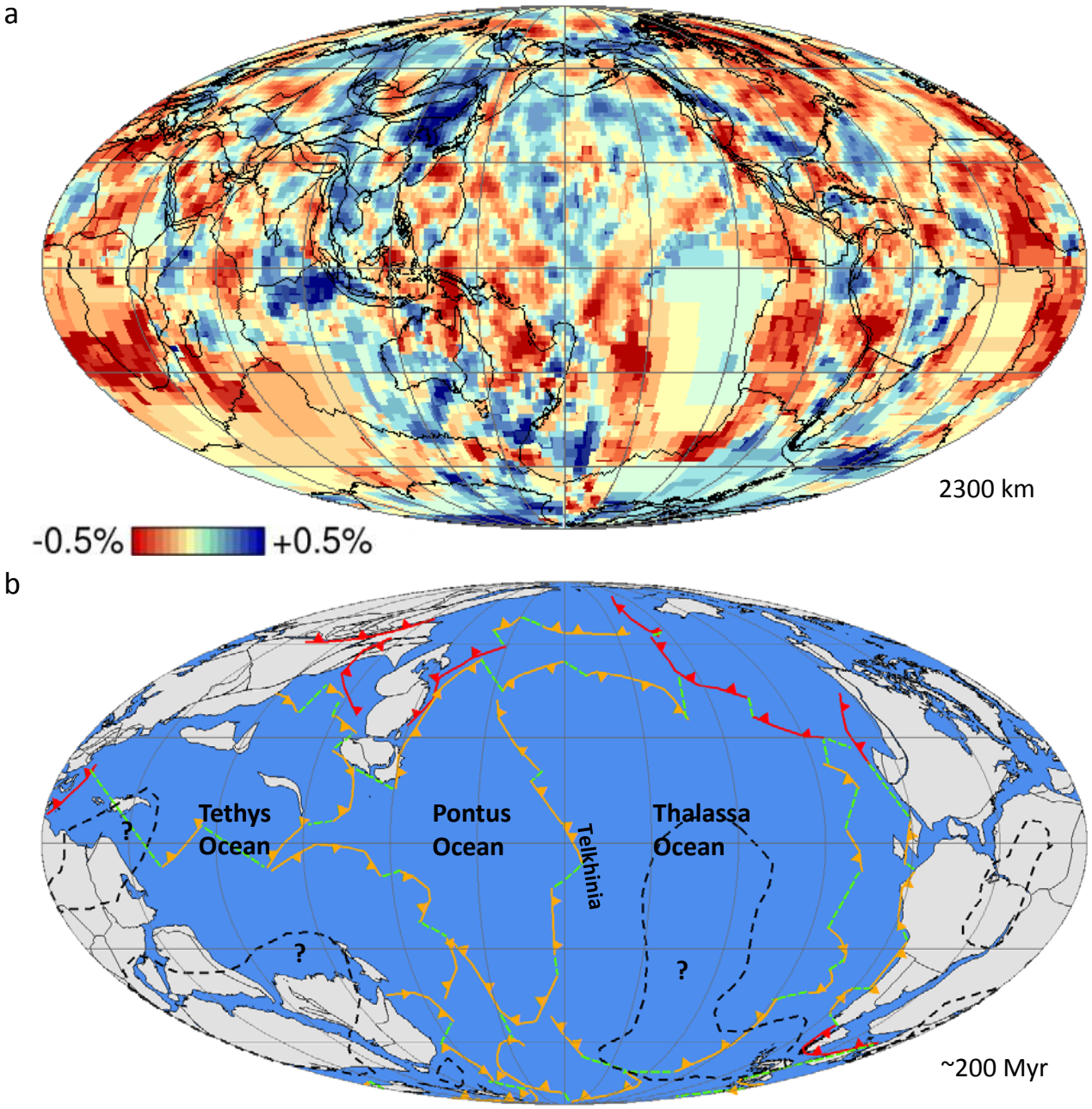

Supplementary Figure 5 Plate tectonic interpretation of tomography. Mollweide projection of a) tomographic depth sliceswith present-day continents at 2300 km and b) plate tectonic interpretation at ~200 Myr. Legend similar as in Supplementary Figure 1.

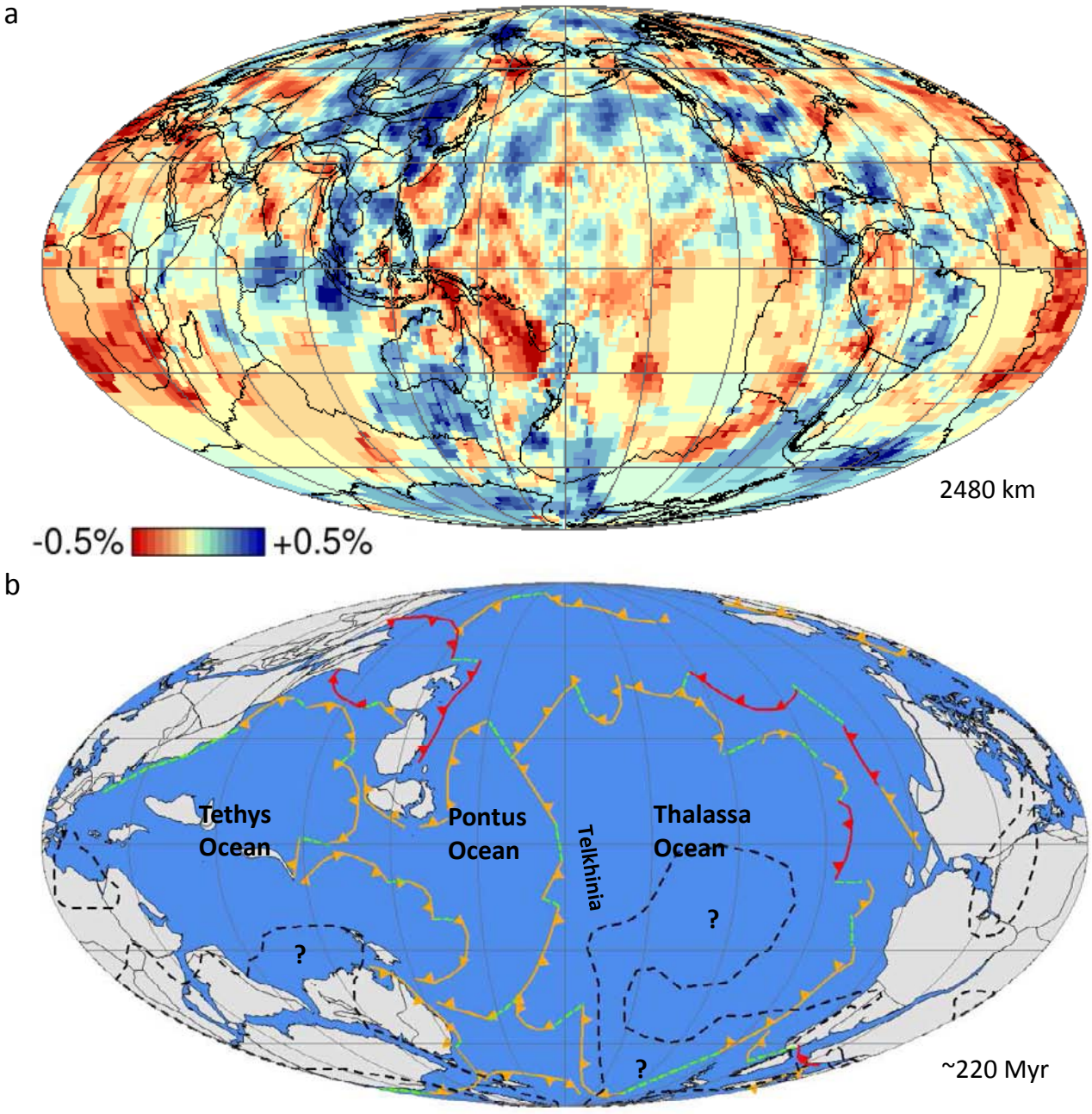

Supplementary Figure 6 Plate tectonic interpretation of tomography Mollweide projection of a) tomographic depth sliceswith present-day continents at 2480 km and b) plate tectonic interpretation at ~220 Myr. Legend similar as in Supplementary Figure 1.

DOI: 10.1038/NGEO1401

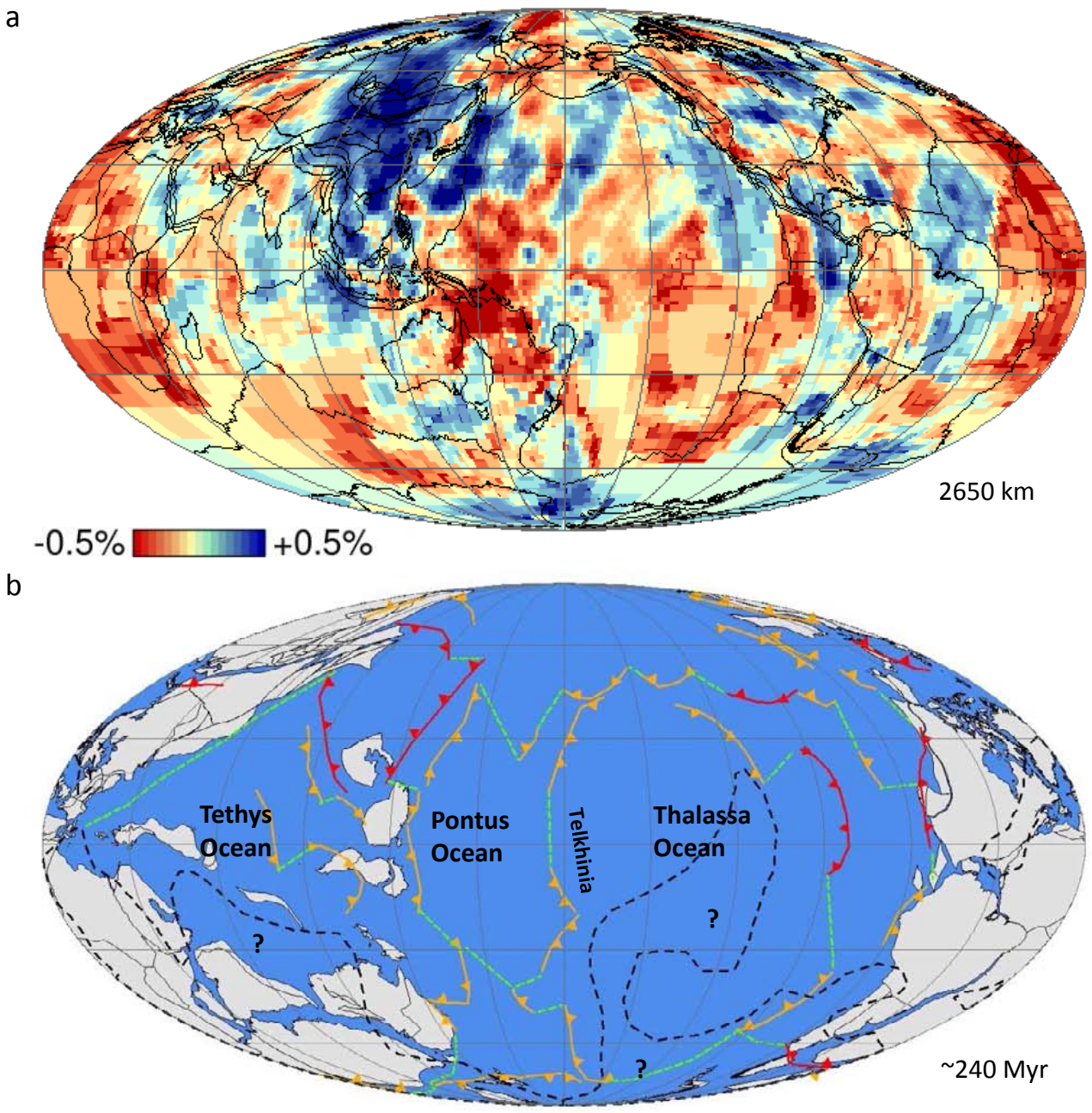

Supplementary Figure 7 Plate tectonic interpretation of tomography Mollweide projection of a) tomographic depth sliceswith present-day continents at 2650 km and b) plate tectonic interpretation at ~240 Myr. Legend similar as in Supplementary Figure 1.

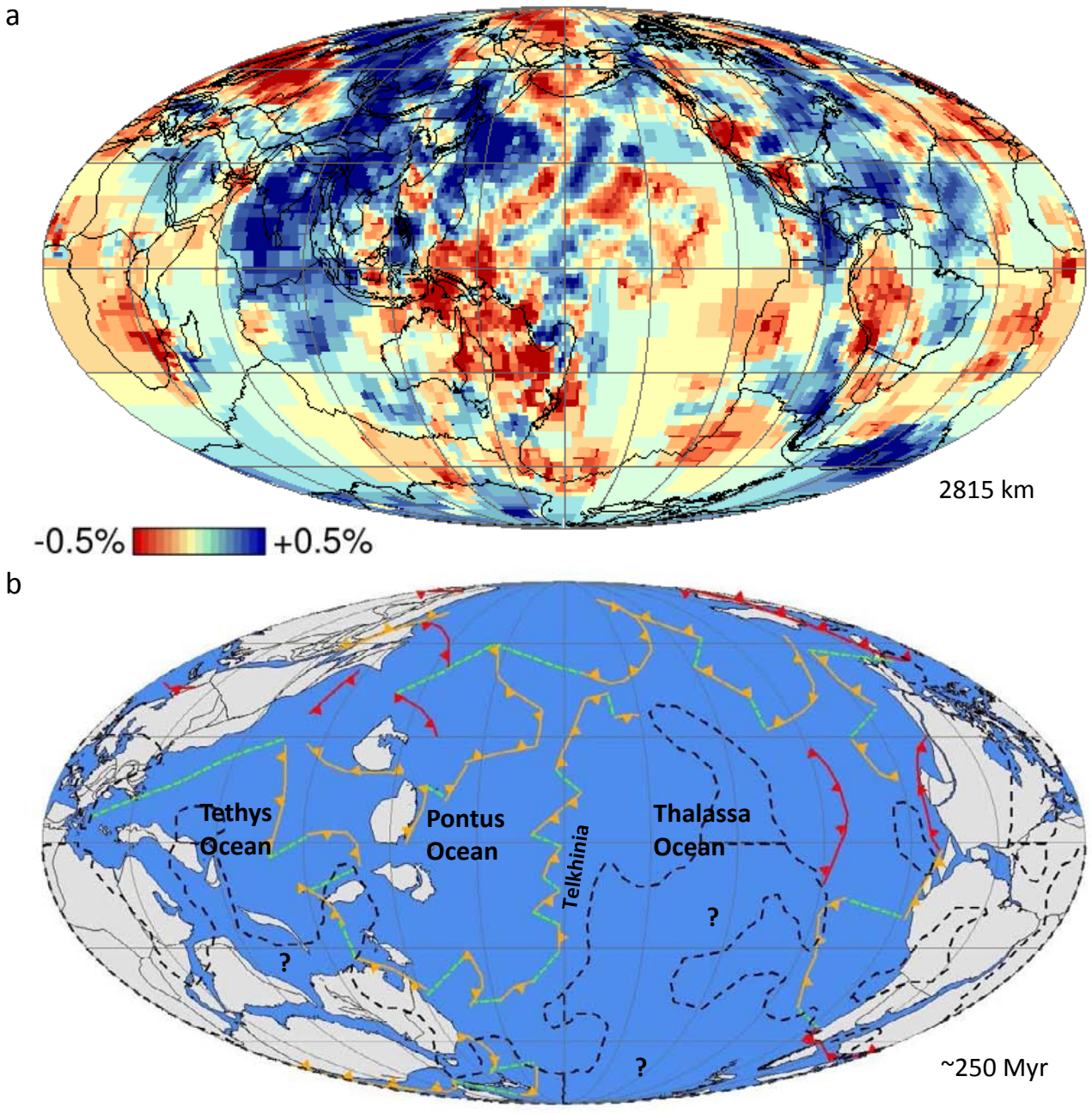

Supplementary Figure 8 Plate tectonic interpretation of tomography Mollweide projection of a) tomographic depth sliceswith present-day continents at 2815 km and b) plate tectonic interpretation at ~250 Myr. Legend similar as in Supplementary Figure 1.

DOI: 10.1038/NGEO1401

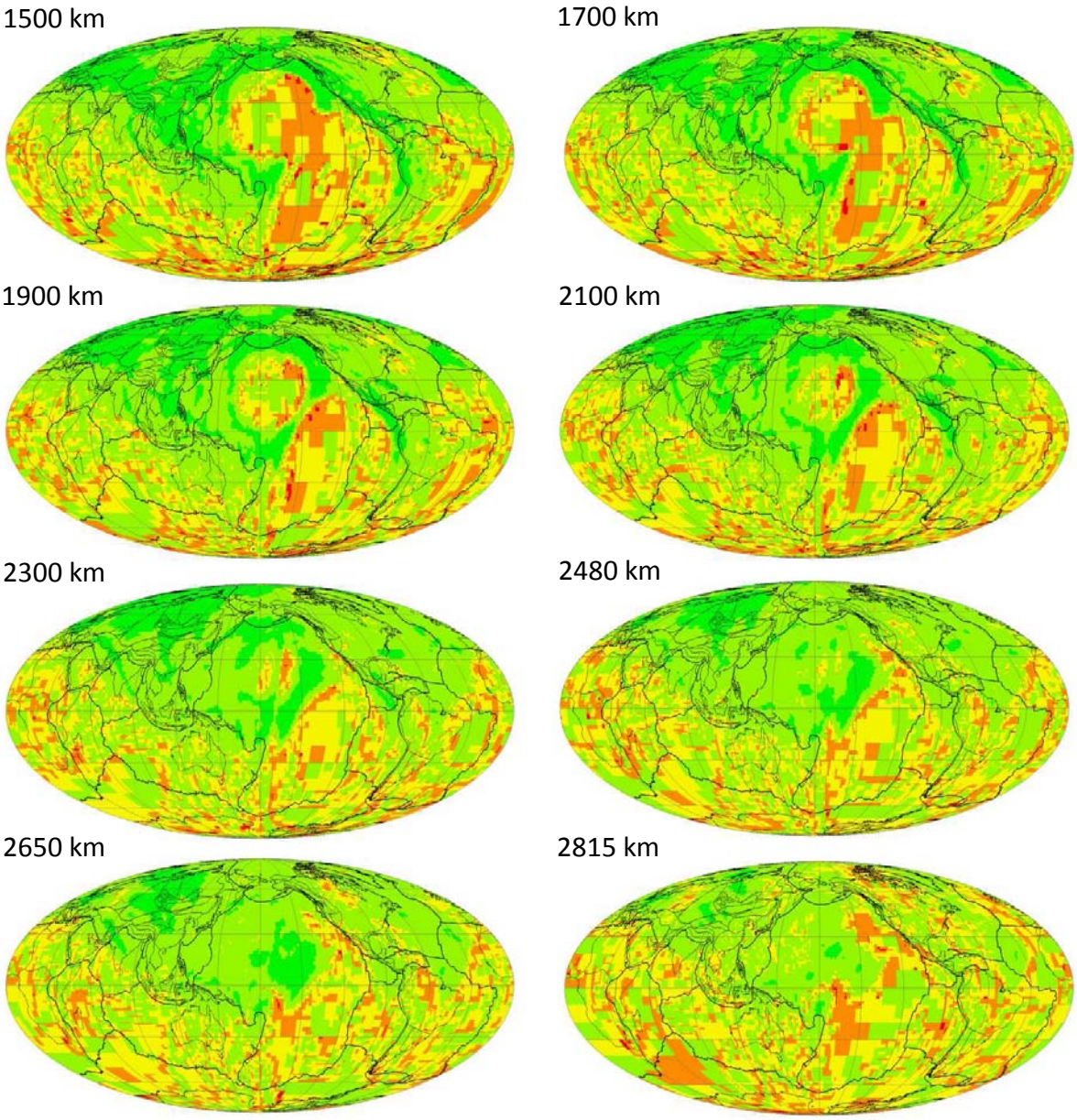

Supplementary Figure 9 Hitcount maps. Mollweide projection of hitcounts. Colour scale is scaled from red (<100 raypaths/cell), orange (100-500), yellow (500-1000), light green (1000-5000), dark green (5000+ raypaths/cell)

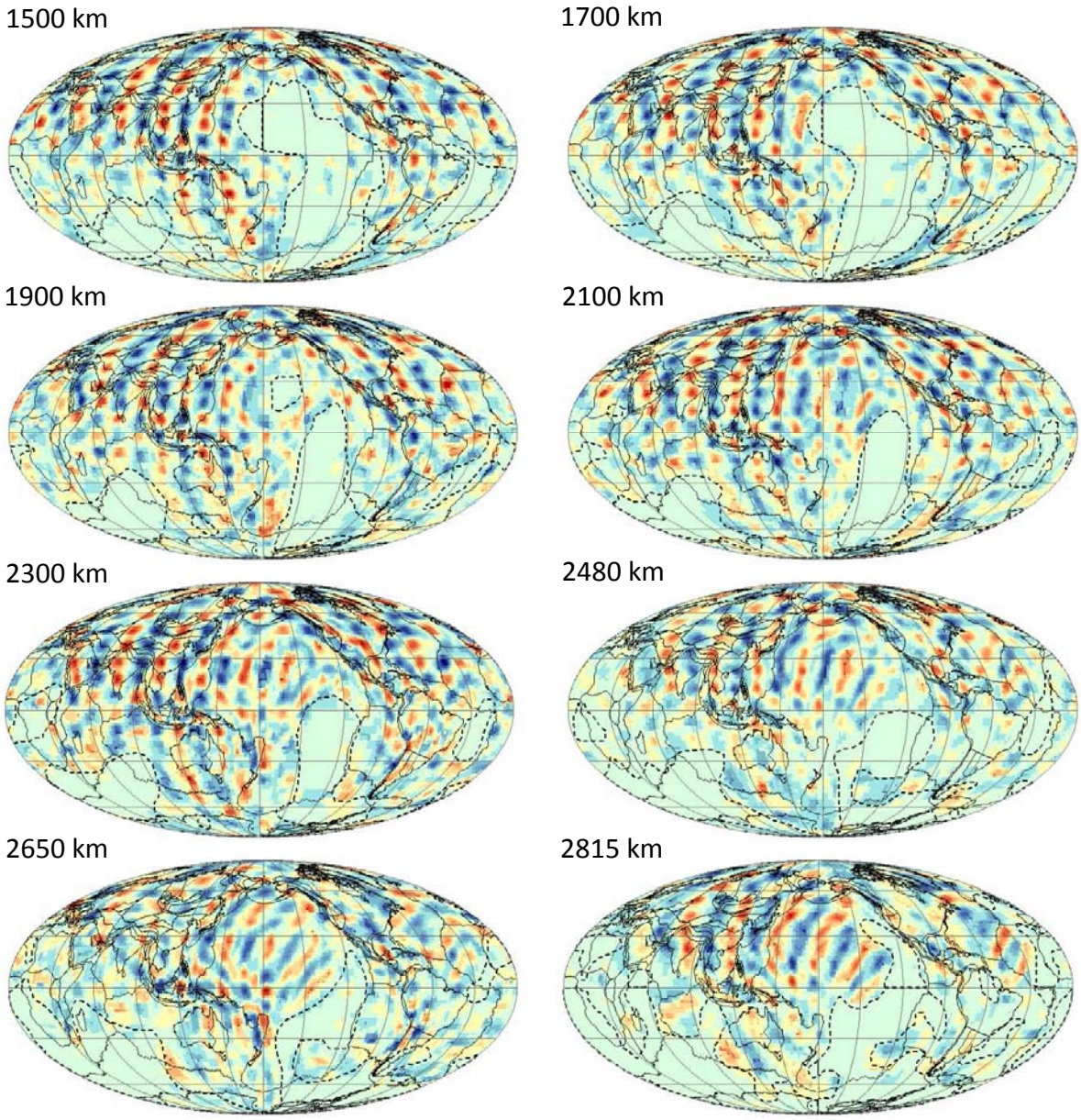

Supplementary Figure 10 Horizontal spike tests. Mollweide projection of spike tests of 5x5 degree cells. Colour scale is scaled from red (-2.5%) to blue (+2.5%). Low resolution zones where the returned amplitudes are near-zero (yellow), are indicated by dashed outlines.